

Applications of GPS Theory and Algorithms

Software development using GPS theory and algorithms is discussed in this chapter. A concept of precise kinematic positioning and flight-state monitoring of an airborne remote sensing system is presented.

10.1 Software Development

GPS/Galileo software consists generally of three basic components: a functional library, a data platform, and a data processing core. The functional library provides all possibly needed physical models, algorithms and tools for use. The data platform prepared all possibly needed data for use and performing the preparation in a time loop. The data processing core forms the observation equations, accumulates them within the time loop and solves the problem if desired. Software can be developed using the theory and algorithms outlined in this reference and handbook.

10.1.1 Functional Library

A functional library consists of physical models, algorithms and tools. For convenience, the functions are listed below with the references referring to the contents described in this book (cf. Figs. 10.1–10.3).

Physical Models

1. Tropospheric models for correcting or determining the tropospheric effects (cf. Sect. 5.2);
2. Ionospheric model for correcting the ionospheric effects (cf. Sect. 5.1);
3. Relativity models for correcting the relativistic effects (cf. Sect. 5.3);
4. Earth tide model for the correction of the tidal displacements of the Earth-fixed stations (cf. Sect. 5.4);
5. Ocean loading tide model for computing corrections of the ocean loading displacements especially for the stations near the coast (cf. Sect. 5.4);
6. Satellite mass centre model for transformation between the mass centre and receiver antenna centre of the GPS satellite (cf. Sect. 5.8);
7. Solar radiation model for orbit determination (cf. Sect. 11.2.4);
8. Atmospheric drag model for LEO orbit determination (cf. Sect. 11.2.5);

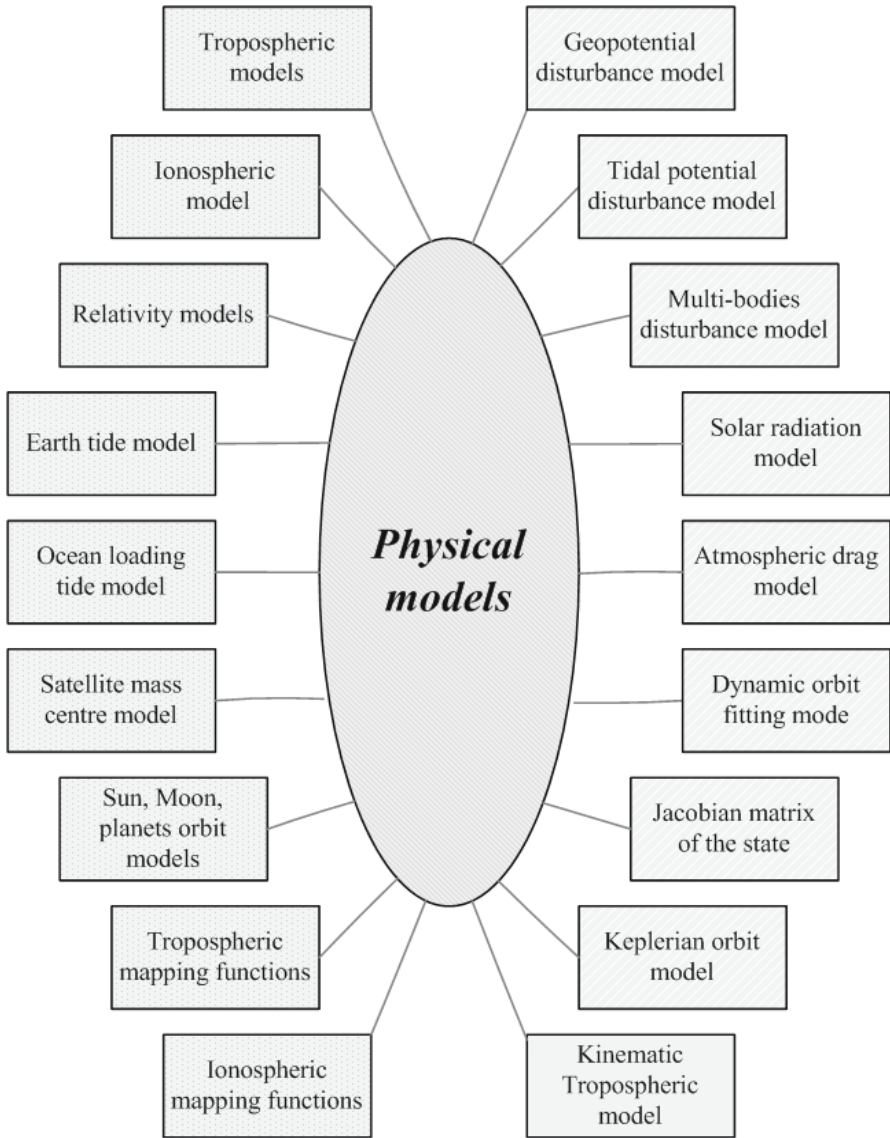


Fig. 10.1. Physical models

9. Geopotential disturbance model for dynamic orbit determination and LEO satellite geopotential determination (cf. Sect. 11.2.1);
10. Tidal potential disturbance model for precise dynamic orbit determination and LEO satellite geopotential determination (cf. Sect. 11.2.3);
11. Multi-body disturbance models for the correction of the perturbations (cf. Sect. 11.2.2);
12. Dynamic orbit fitting model for orbit correction in a regional network (cf. Sect. 11.4);

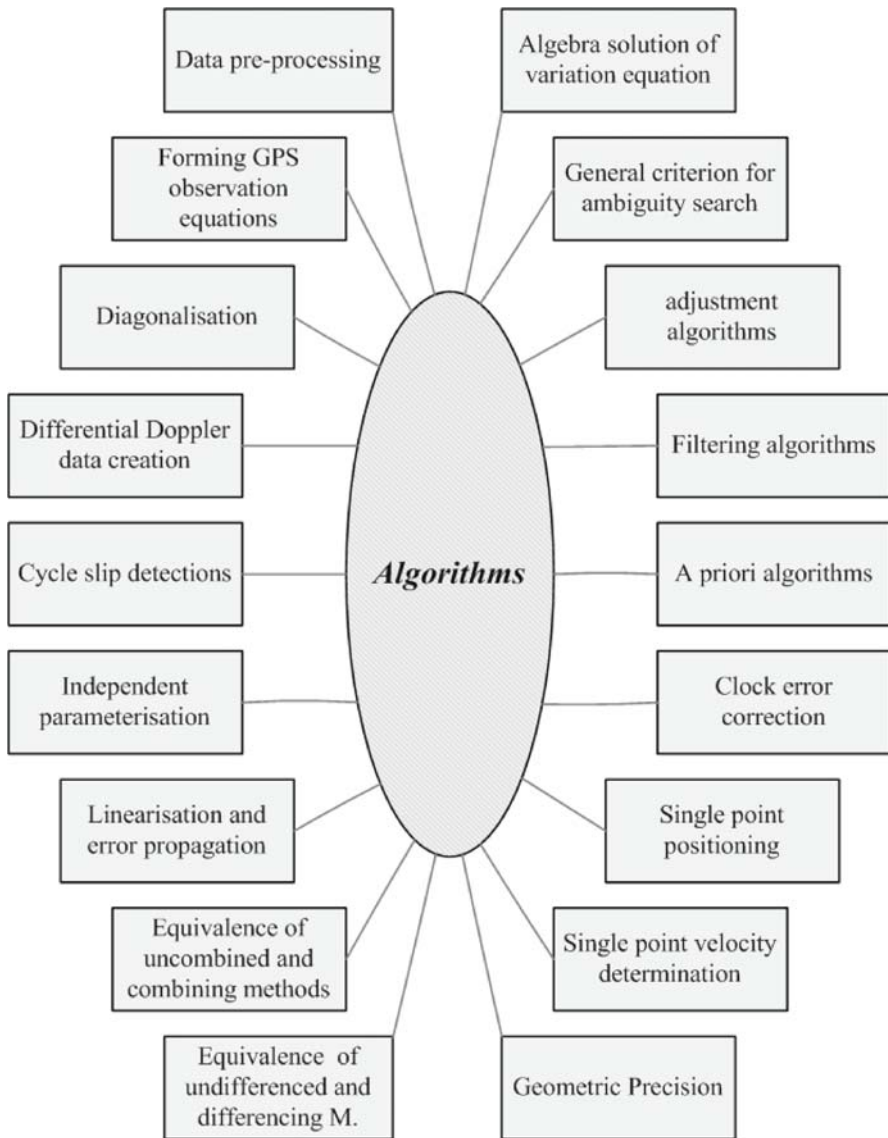


Fig. 10.2. Algorithms

13. Sun, Moon, and planet orbit models for computing the ephemerides of the Sun, Moon and planets, the multi-body disturbance and the Earth tide effects (cf. Sects. 11.2.8, 11.2.2 and 5.4);
14. Tropospheric mapping functions (cf. Sect. 5.2);
15. Ionospheric mapping functions (cf. Sect. 5.1);
16. Tropospheric model for kinematic receiver (cf. Sect. 10.2.2);
17. Keplerian orbit model (cf. Sect. 3.1.3);

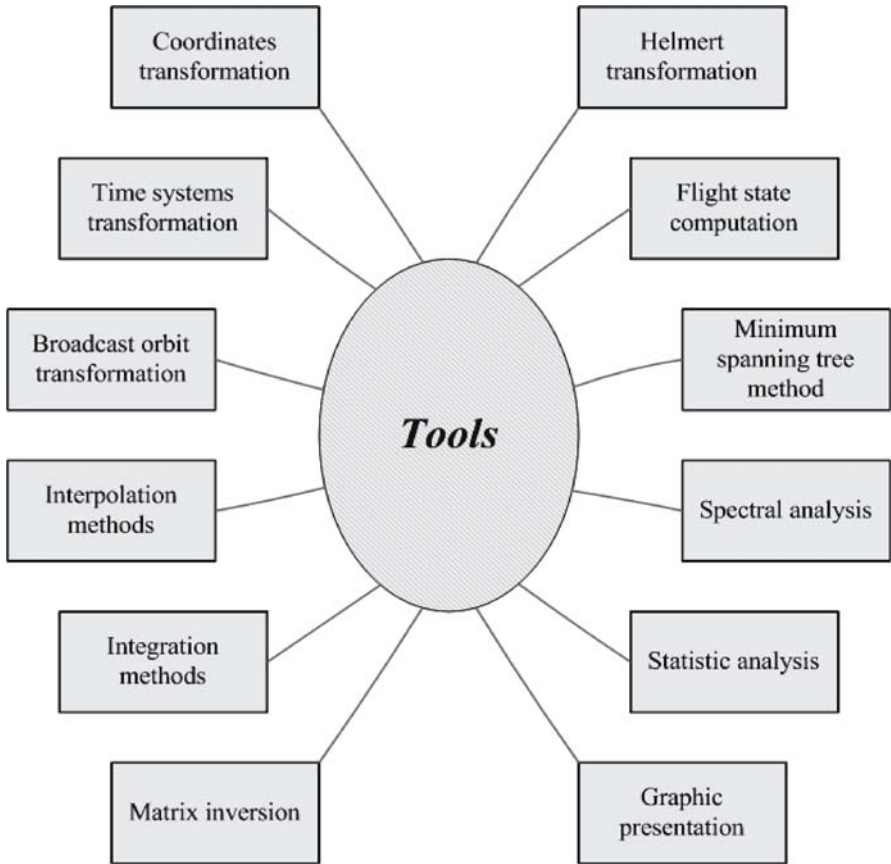


Fig. 10.3. Tools

18. Jacobian matrices of the Keplerian elements and the state vector of the satellite (cf. Sects. 3.1.1, 3.1.2, 3.1.3, 11.3 and 11.7).

Algorithms

1. Data pre-processing (cf. Sect. 9.4.1);
2. Forming GPS observation equations (cf. Sects. 4.1, 4.2, 4.3 and 6.1);
3. Differential Doppler data creation if necessary (cf. Sect. 6.5.5);
4. Cycle slip detections (cf. Sect. 8.1);
5. Independent parameterisation algorithms (cf. Sect. 9.1);
6. Linearisation and covariance propagation (cf. Sects. 6.3, 6.4, 11.5 and 11.7);
7. Equivalent algorithms of uncombined and combining methods (cf. Sects. 6.5, 6.7 and 9.2);
8. Equivalent algorithms of undifferenced and differencing algorithms (cf. Sects. 6.6, 6.8, 7.6 and 9.2);
9. Diagonalisation algorithm (cf. Sects. 7.6.1 and 9.1);

10. Algebraic solution of the variation equation (cf. Sect. 11.5.1);
11. Ambiguity search using general and equivalent criteria (cf. Sect. 8.3);
12. Classical adjustment tools (Least Squares adjustment (LSA), sequential LSA, conditional LSA, block-wise LSA, and equivalent algorithms, cf. Sects. 7.1–7.5);
13. Filtering algorithms (Kalman filter, robust Kalman filter, and adaptive robust Kalman filter, cf. Sects. 7.7.1, 7.7.2 and 7.7.3);
14. A priori constrained LSA (cf. Sects. 7.8.1 and 7.8.2);
15. Clock error corrections (cf. Sect. 5.5);
16. Single point positioning (cf. Sect. 9.4.2);
17. Single point velocity determination (cf. Sect. 9.4.6);
18. Accuracy of the observational geometry (cf. Sect. 9.5).

Tools

1. Coordinate transformation tools (cf. Sects. 2.1, 2.3, 2.4 and 2.5);
2. Time system transformation functions (cf. Sect. 2.6);
3. Broadcast orbit transformation in IGS format (cf. Sect. 3.3);
4. Interpolation tools (cf. Sects. 3.4, 5.4.2 and 11.6.5);
5. Integration methods (cf. Sects. 11.6.1, 11.6.2, 11.6.3 and 11.6.4);
6. Matrix inverse functions (Gauss-Jordan and Cholesky algorithms)
7. Helmert transformation (cf. Sect. 2.2);
8. Flight state computation (cf. Sect. 10.2.3);
9. Minimum spanning tree method for forming optimal baseline network (cf. Sect. 9.2);
10. Spectral analysis methods (cf. Xu 1992);
11. Statistic analysis (cf. Sects. 6.4 and 7.2);
12. Graphic representation.

10.1.2

Data Platform

A data platform consists of three parts: the common part, the sequential time loop part, and the summary part. For convenience, the functions are listed below with the references referring to the contents described in this book (cf. Fig. 10.4).

Common Part

1. Program start;
2. Read input parameter file for controlling the run of the software (an example of the definition of the input parameter file, cf., e.g., Xu 2004);
3. Read all possible data files necessary for the run of the software (e.g., satellite information file, station information file, geopotential data file, ocean loading coefficients, GPS orbit data file, polar motion data file, etc.);
4. Read or create the Sun-Moon-planet orbit data;
5. Compute Earth/ocean loading tide displacements;
6. GPS satellite orbit data transformation if necessary;
7. Data pre-processing if possible;
8. Optimal baseline network construction and initialisations.

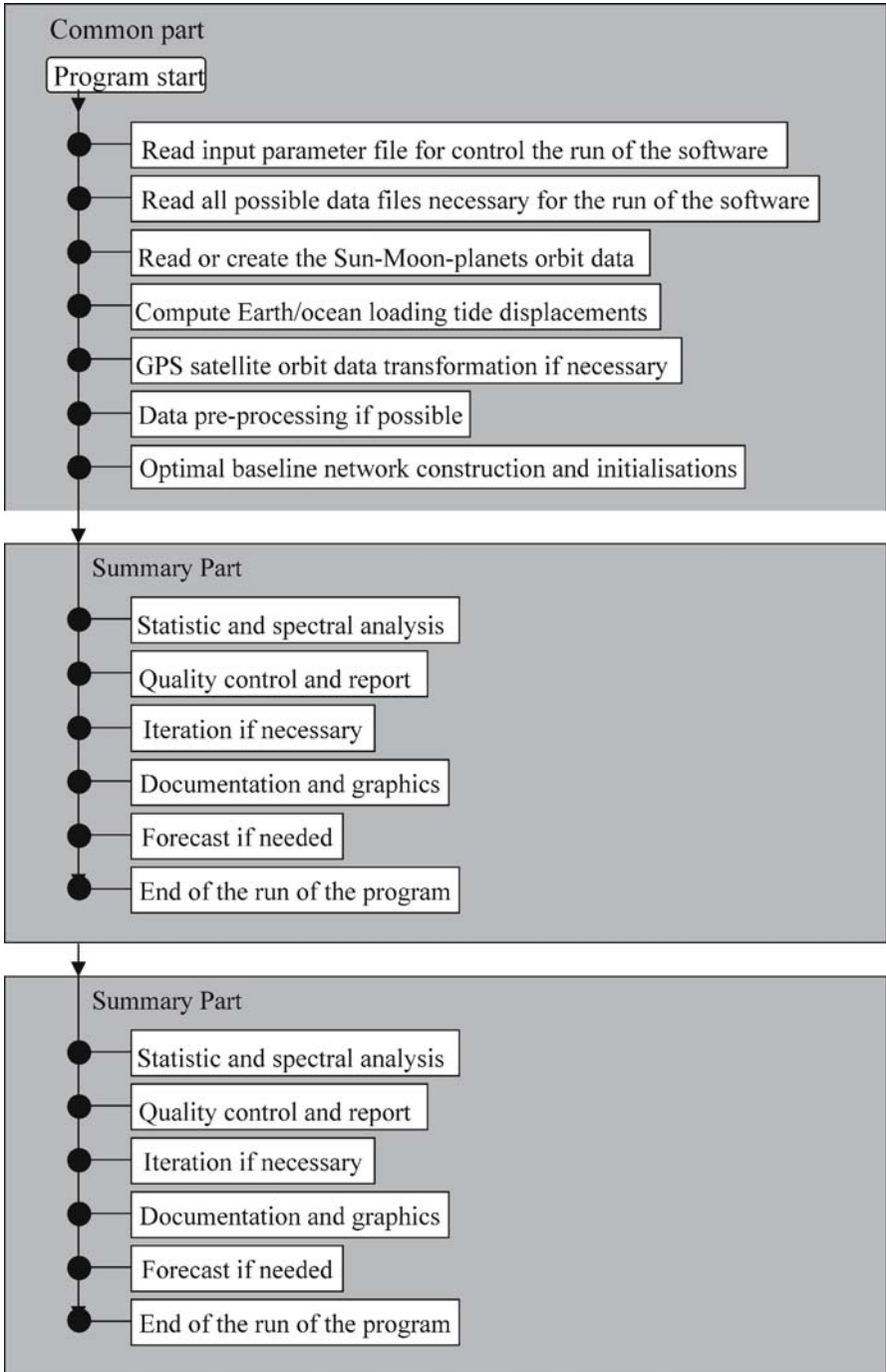


Fig. 10.4. Program common part, sequential time loop part, summary part

Sequential Time Loop Part

1. Sequential time loop start;
2. Get the needed data for use at the related epoch (e.g., initial coordinates of the receivers, etc.);
3. Compute all possible parameters and model values for use at the related epoch (e.g., transformation matrices, interpolated orbit data, values of correcting models, etc.);
4. Read the GPS observation data and transform to a suitable form for use;
5. Single point positioning (e.g., for the second type of clock error correction);
6. Single point velocity determination (velocity belongs to the state vector of the station);
7. Data processing core (cf. Sect. 10.1.3);
8. End of the sequential time loop.

Summary Part

1. Statistic analysis and spectral analysis of the results;
2. Quality control and report;
3. Iteration if necessary;
4. Documentation and graphic representation;
5. Forecast if needed;
6. End of the run of the program.

10.1.3

A Data Processing Core

A data processing core is a collection of GPS data processing algorithms controlled by switches. Based on the above functional library and data platform, to realise a specific function of GPS software turns out to be a relatively simple job – one just needs to construct the function and add it to the data processing core. A multifunctional data processing core is a collection of individual functions and can be switched from one to the other through input parameters. Therefore, a data processing core is a list of specific program functions with switches. A specific function can be called a sub-core, which is dependent on the specific purposes of the data processing. Indeed the single point positioning and velocity determination functions are two functions of the data processing core. A list of the possible functions of a multifunctional data processing core and a structure of a sub-core are given below as examples.

Functions of a Multi-Functional Data Processing Core

1. Single point state vector determination for static and kinematic as well as dynamic applications;
2. Relative positioning for static and kinematic applications;
3. Ionosphere and atmosphere soundings;
4. Regional tectonic monitoring with orbit corrections;
5. Global network positioning and GPS orbit determination;
6. LEO orbit determination and geopotential determination.

Structure of a Sub-Core

1. Computing the computed observables using the orbit and station data as well as the values of the physical models (may be used for system simulation);
2. Computing the coefficients of linearised observation equations;
3. In the case of dynamic applications, solving the variance equations for forming the orbit related observation equations;
4. Forming the normal equations;
5. Accumulation of the normal equations;
6. Solving the problem if desired.

10.2

Concept of Precise Kinematic Positioning and Flight-State Monitoring

A concept of precise kinematic positioning and flight-state monitoring of an airborne remote sensing system is presented here, based on the practical experiences from the EU project AGMASCO. Within the project, about two months of kinematic GPS flight data and static reference data have been collected in Europe over four campaigns during three years. An independently developed GPS software package and several commercial GPS software packages have been used for data processing. In this chapter, the methods of creating the tropospheric model for the aircraft trajectory and the use of static ambiguity results as conditions in the kinematic positioning are discussed. These concepts are implemented in the kinematic/static GPS software KSGsoft, and they have demonstrated excellent performance (cf. Xu 2000).

10.2.1

Introduction

The EU (European Union) project AGMASCO (Airborne Geoid Mapping System for Coastal Oceanography), in which five European institutions participated, has collected about two months of multiple static and airborne kinematic GPS data for the purpose of kinematic positioning and flight state monitoring of an airborne remote sensing system. The remote sensing system includes an aerogravimeter, accelerometer, radar and laser altimeter, INS and datalogger. During the project, four flight campaigns were performed in Europe (Fig. 10.5). They were the test campaign in Braunschweig in June 1996 (Fig. 10.6), the Skagerrak campaign in September 1996 (Fig. 10.7), the Fram Strait campaign in July 1997 (Fig. 10.8) and the Azores campaign in October 1997 (Fig. 10.9). Two to three kinematic GPS antennas were mounted on the fuselage, the back and the wing of the aircraft, and at least three GPS receivers were used as static reference receivers.

The above-mentioned remote sensing system has two very important objectives: to measure the gravity acceleration of the Earth and to determine the sea surface topography. Because the aerogravimeter (or accelerometer) and the altimeter are firmly attached to the aircraft, kinematic positioning and flight-state monitoring using GPS plays a key role for determining the flight acceleration, velocity and position, as well as orientation of the aircraft. The high sensitivity of the sensors requires high quality aircraft positioning and flight-state monitoring. Therefore, new strate-

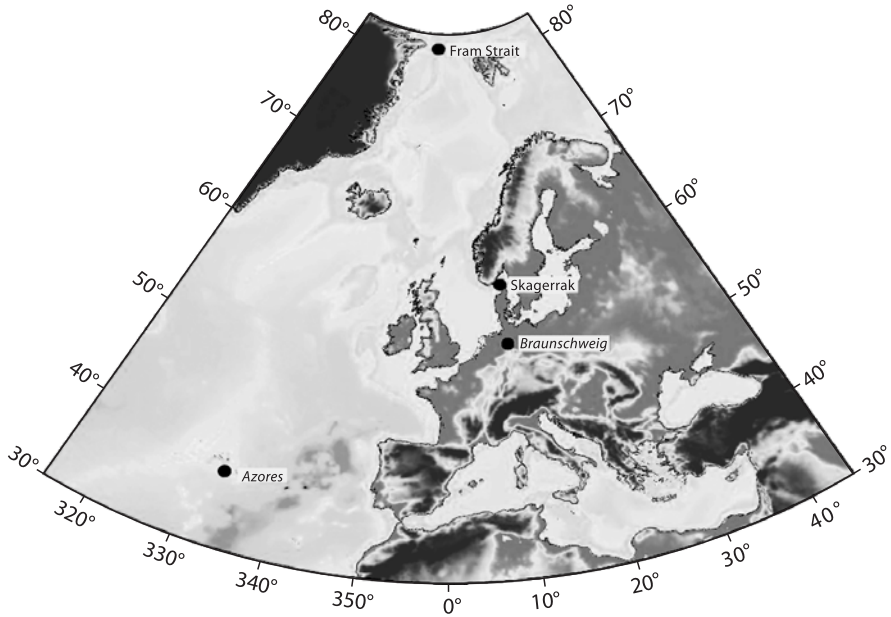


Fig. 10.5. Measured areas of the four flight campaigns

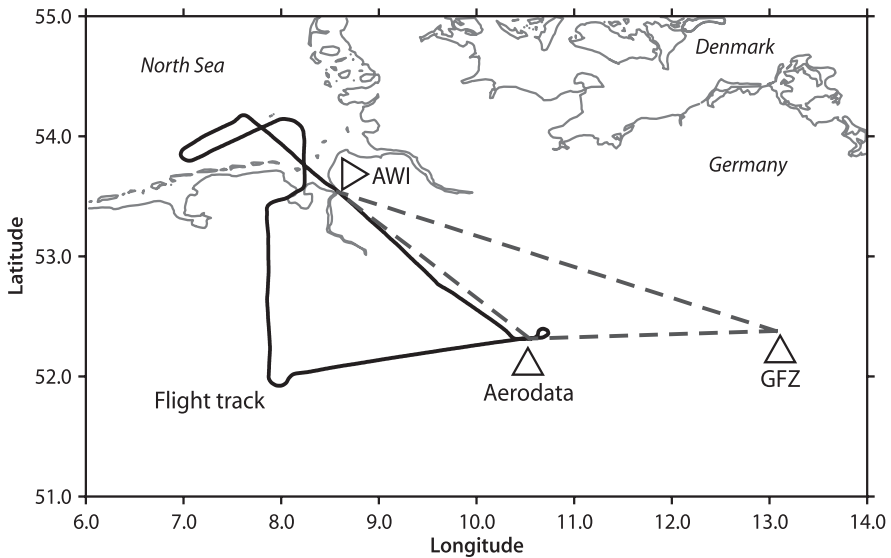


Fig. 10.6. Flights in the Braunschweig campaign (June 1996)

gies and methods have been studied, developed, tested and implemented for GPS data processing.

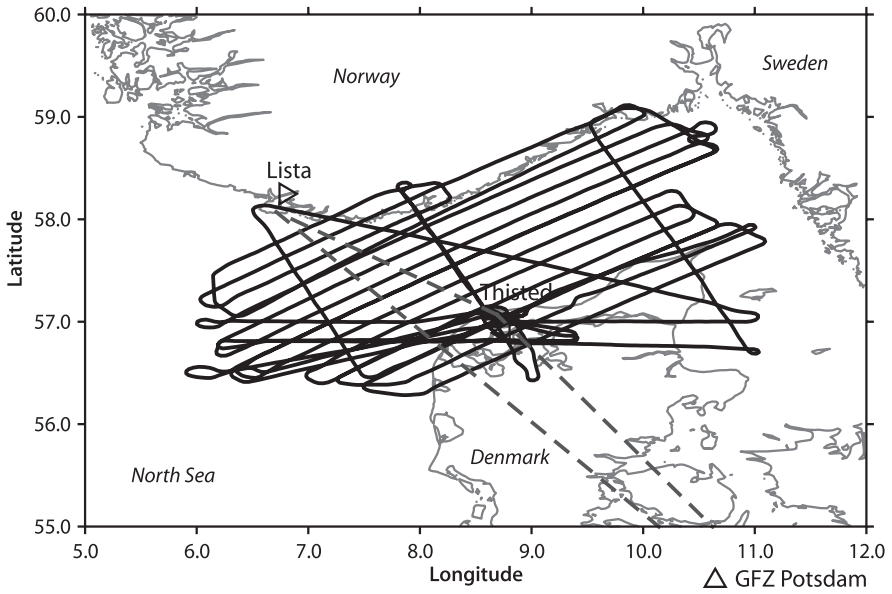


Fig. 10.7. Flights in the Skagerrak campaign (September 1996)

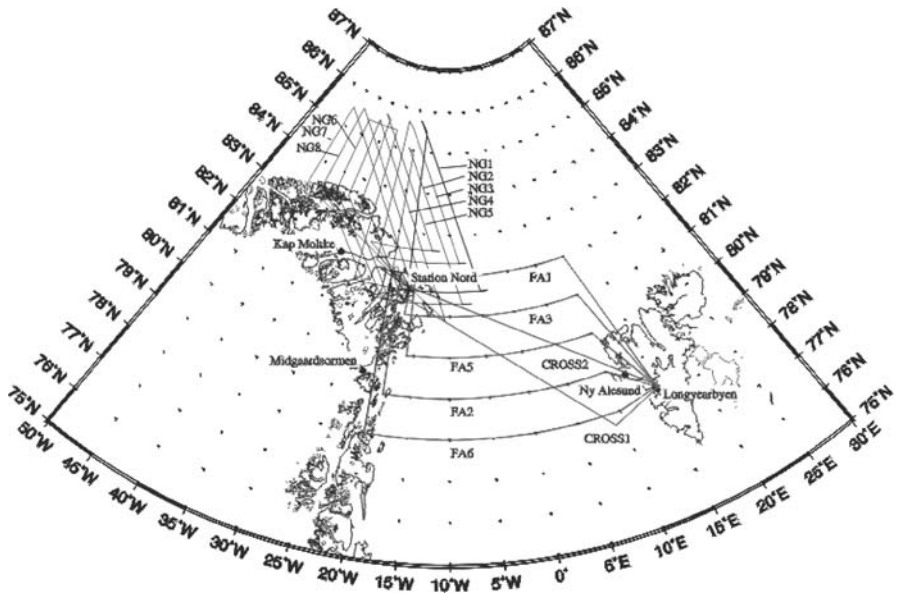


Fig. 10.8. Flights in the Fram Strait campaign (July 1997)

The adopted concept of precise kinematic positioning and flight-state monitoring are discussed in Sects. 10.2.2 and 10.2.3, respectively.

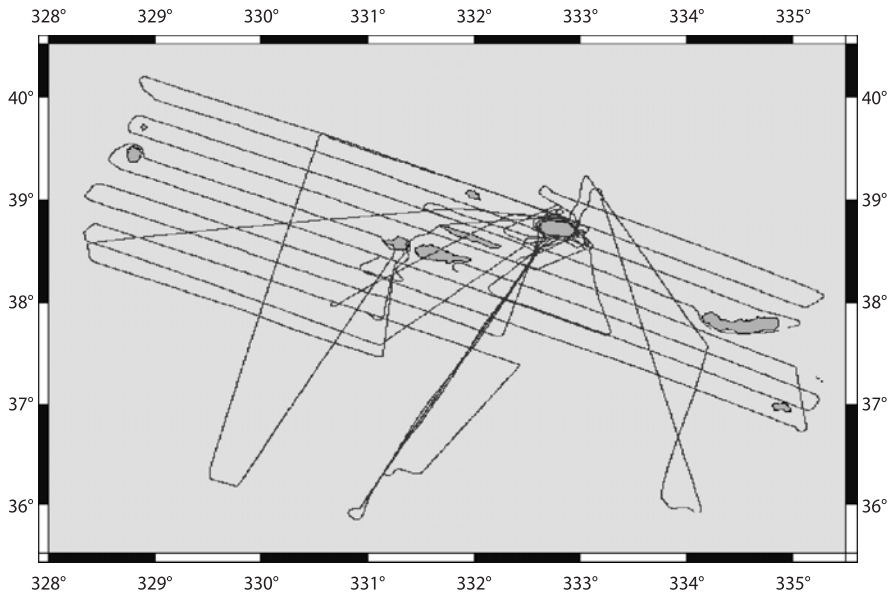


Fig. 10.9. Flights in the Azores campaign (October 1997)

10.2.2

Concept of Precise Kinematic Positioning

A vast literature exists on the topic of precise kinematic positioning (see, e.g., Goad and Remondi 1984; Wang et al. 1988; Schwarz et al. 1989; Cannon et al. 1997; Hofmann-Wellenhof et al. 1997). Based on AGMASCO practice, a modified concept has been developed and applied to data processing.

10.2.2.1

Combining the Static References with IGS Station

It is well-known that differential GPS positioning results depend on the accuracy of the reference station(s). However, it is not quite clear how strong this dependency is, or in the other words, how accurate the reference coordinates should be determined for use in kinematic differential positioning. During AGMASCO data processing, it was noticed that the accuracy of the reference coordinates is very important. A bias in the reference station coordinates will cause not only a bias in the kinematic flight path, but also a significant linear trend. Such a linear trend depends on the flight direction and the location of the reference receiver(s). Therefore, in precise kinematic positioning, the coordinates of the static reference station should be carefully determined by, for example, connecting these stations to the nearby IGS stations. A detailed study of the relationship between the accuracy of the reference station coordinate and the quality of kinematic and static positioning has been carried out by Jensen (1999).

10.2.2.2
Earth Tide and Loading Tide Corrections

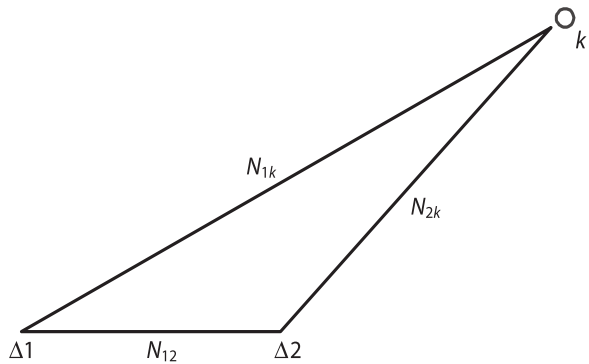
A detailed study of the Earth tide effects on GPS kinematic/static positioning is given in Xu and Knudsen (2000). For airborne kinematic differential GPS positioning, Earth tide effects on the static reference station need to be corrected for. Such tidal effects could reach up to 30 cm in Denmark and Greenland, and 60 cm at other locations in the world. Tidal effects could induce a “drift” over a few hours of measurement duration. For ground-based kinematic and static differential GPS positioning with baseline lengths less than 80 km, the impact of the Earth tide effects could reach more than 5 mm. In precise application of GPS positioning, both in kinematic and static cases, the Earth tide effects have to therefore be taken into account even for a relatively small local GPS network.

Ocean loading tide effects could also reach up to a few cm in magnitude, in special cases (Ramatschi 1998). Generally, ocean loading tide effects should be considered at the cm level in coastal areas, so that these effects have to be corrected for GPS data processing. However, unlike the Earth tide, ocean loading tide effects can only be modelled by ocean tide models at about 60% to 90% (Ramatschi 1998). Therefore, simply using a model to correct for the effects is not enough, and a detailed study of ocean loading tide effects is necessary for precise positioning. It is, however, possible to use GPS for determining the parameters of the local ocean loading tide effects (Khan 1999).

10.2.2.3
Multiple Static References for Kinematic Positioning

In differential GPS kinematic positioning, usually there is only one static reference used. It is obvious that if multiple static references are used, the reference station dependent errors, such as those due to the troposphere and ionosphere as well as ocean loading tide effects, could be reduced and the geometric stability could be strengthened. For simplicity, only the case of using two static reference receivers will be discussed here. In Fig. 10.10, 1 and 2 denote the static reference receivers, and k denotes the kinematic object. Suppose the two static stations are placed close by and both have the same GPS satellites in view. Using one static reference receiver for kinematic positioning, one has unknown vector $(X_k \ N_{1k})$, where X is the coordinate sub-vector and N is the ambiguity sub-vector. Using two static references, one has unknown

Fig. 10.10.
 Multiple static references for kinematic positioning



vector $(X_k \ N_{1k} \ N_{2k})$, because the unknown coordinate sub-vector X is the same. The number of elements of the sub-vector N compared with that of X is very small in the kinematic case. Therefore, by using multiple static reference receivers for kinematic positioning, the total number of observations is increased, but the total number of unknowns remains almost the same; hence the results will be modified.

Furthermore, according to the definition of double differenced ambiguities, one has

$$N_{1k} = N_1^j - N_k^j - N_1^J + N_k^J, \quad (10.1)$$

$$N_{2k} = N_2^j - N_k^j - N_2^J + N_k^J \quad (10.2)$$

and

$$N_{12} = N_1^j - N_2^j - N_1^J + N_2^J, \quad (10.3)$$

where N on the right sides is un-differenced ambiguity, indices j and J denote satellites, 1 and 2 denote the static stations, and k denotes the kinematic station. Then one gets

$$N_{1k} - N_{2k} = N_{12}, \quad (10.4)$$

where N_{12} is the double difference ambiguity vector of the static baseline, which can be obtained from the static solution. Using relation Eq. 10.4, N_{2k} can be represented by $(N_{1k} - N_{12})$. Thus, using two static references for kinematic positioning, one has nearly doubled the number of observables, yet the unknowns remain the same, if in addition the static results are used. (Usually static measuring can be made over a longer time, and hence the static results can be obtained precisely).

In the case of a single difference, one has

$$N_{1k} = N_1^j - N_k^j, \quad (10.5)$$

$$N_{2k} = N_2^j - N_k^j, \quad (10.6)$$

and

$$N_{12} = N_1^j - N_2^j, \quad (10.7)$$

where N on the right sides is un-differenced ambiguity, index j denotes the satellite, 1, 2 denote the static stations, and k denotes the kinematic station. Then one gets the same relation as in the case of double difference:

$$N_{1k} - N_{2k} = N_{12}. \quad (10.8)$$

For un-differenced data processing, ambiguity vectors are $(N_1^j \ N_k^j)$ and $(N_2^j \ N_k^j)$ in kinematic data processing using a single reference. $(N_1^j \ N_2^j)$ is the ambiguity vector in static data processing. No matter how one deals with the reference-related ambiguities, the common part of ambiguities obtained from static data processing can be used in kinematic data processing.

Using multiple static reference receivers and introducing the ambiguities from the static solution as conditions, the accuracy of the kinematic positioning can be increased significantly. An example showing the differences in the height of the front antenna determined using multiple reference receivers, with and without using the static ambiguity condition, is given in Fig. 10.14 (the ambiguity float solutions are used). The average and standard deviation of the differences are 27.07 and 4.34 cm, respectively. These results clearly indicate that the multiple static conditions have modified the results. A change of ambiguity not only caused a bias in the position solution, but also a high frequency variation. The base-base separation is about 200 km, and the length of the kinematic path is about 400 km (cf. Fig. 10.9).

For three or more static references receivers, similar arguments and improved results can be presented.

10.2.2.4

Introducing Height Information as a Condition

Even after using multiple static reference receivers and the static conditions, the ambiguities in kinematic positioning can still be wrong. In such a case, there could be a bias and a variation in the kinematic trajectory (see Sect. 10.2.4.2 and Fig. 10.14). Therefore, introducing the height information of the aircraft at the start and/or resting point into the data processing is a great help, especially in the airborne altimetry applications. The bias of the results obtained by using different software can then be eliminated.

10.2.2.5

Creation of a Kinematic Tropospheric Model

Using the multiple static reference receivers, the parameters of the tropospheric model can be determined. Using these parameters, the tropospheric model parameters for the kinematic receiver can be interpolated. Such a model, however, generally is only suitable for the footprint point of the kinematic platform. Therefore, the vertical gradient of temperature and the exponential changes of pressure and humidity (Syndergaard 1999) are introduced into the standard model to create a tropospheric model for the kinematic station in the air. This is, of course, not an ideal model; however, it is a very reasonable one.

10.2.2.6

Higher Order Ionospheric Effect Correction

For long distance kinematic positioning, the ionosphere-free combination has to be used to eliminate the ionospheric effects. It is well-known that the ionosphere-free combination is indeed only a first order approximation (Klobuchar 1996). The second order ionospheric effects are about 0.1% of that of the first order (Syndergaard 1999). Therefore the residual ionospheric effects can reach the level of a few cm. This has to be taken into account by using some form of modelling of the total ionospheric effects.

10.2.2.7

A General Method of Integer Ambiguity Fixing

An integer ambiguity search method based on the conditional adjustment theory was proposed in Sect. 8.3. This method has been implemented in the GPS software KSGsoft (Kinematic/Static GPS Software), developed in GFZ Potsdam (Xu et al. 1998), and used extensively for real data processing in the EU project AGMASCO (Xu et al. 1997). The search can be carried out in the coordinate domain, ambiguity domain or both domains. Most other least squares ambiguity search methods (Euler and Landau 1992; Teunissen 1995; Merbart 1995; Han and Rizos 1995, 1997) are special cases of this algorithm, if only the ambiguity search domain is selected and without considering the uncertainty of the coordinates caused by ambiguity fixing. By taking the coordinate and ambiguity residuals into account, a general criterion for ambiguity searching is proposed to ensure an optimal search result. Detailed formulas are derived and their usage can be found in Sect. 8.3. The theoretical relationship between the general criterion and the least squares ambiguity search criterion is also derived and illustrated by numerical examples in Sect. 8.3.

10.2.3

Concept of Flight-State Monitoring

For flight-state monitoring of an aircraft, it is necessary that several GPS antennas have to be used. The relative positions between the multiple antennas should be determined. Using, as an example, the method presented in Sect. 10.2.2, the position and velocity of one of the kinematic antennas can be determined. Using this point as a reference, the related position differences of other antennas can be determined. Because the distances between the multiple antennas are only a few meters, the atmospheric and ionospheric effects are nearly identical, and therefore only the single frequency L1 observations are needed for relative positioning. In addition, due to the short ranges, such relative positioning can be performed with high accuracy.

Early stage tests of multiple kinematic GPS antennas mounted on a platform were made for checking purposes, using the known baseline length. Typically, such checks indicate that the distance has a systematic bias if the distance is computed from the two positions and these two positions are determined separately. However, a combined solution of multiple kinematic positioning does not overcome the distance bias problem completely because of inaccuracies in the ambiguity solution. Therefore, for precise flight-state monitoring, it is necessary to introduce the known distances between the antennas fixed on the aircraft as additional constraints in the data processing.

The distance condition can be represented as

$$\rho = \sqrt{(\Delta X)^2 + (\Delta Y)^2 + (\Delta Z)^2}, \quad (10.9)$$

where ΔX , ΔY and ΔZ are the coordinate differences between two antennas, and ρ is the distance. Because of the short distances, the linearisation of the condition cannot be done precisely in the initial step, and therefore an iterative process has to be used. The conditions can be used in a conditional adjustment, or the conditions can be used for eliminating unknowns. Both methods are equivalent.

Flight-state is usually represented by so-called “state angles” (heading, pitch, and roll). They are rotation angles between the body and the local horizontal coordinate frames of the aircraft. The axes of the local horizontal frame are selected as follows: the x^b axis points out the nose, the y^b axis points to the right parallel to the wing, and the z^b axis points out the belly to form a right-handed coordinate system, where b denotes the body frame. The body frame can be rotated to be aligned to the local horizontal frame in a positive, right-handed sense, which is outlined in three steps. First, the body frame is rotated about the local vertical downward axis z by angle ψ (heading). Then the body frame is rotated about the new y^b axis by angle θ (pitch). Finally, the body frame is rotated about the new x^b axis by angle ϕ (roll). In the local horizontal coordinate system, the heading is the azimuth of axis x^b of the body frame, the pitch is the elevation of axis x^b of the aircraft and the roll is the elevation of axis y^b of the aircraft. Note that the directions of the axis x^b and the velocity vector of aircraft are usually not the same. Through kinematic positioning, the three flight state monitoring angles can be computed (Cohen 1996).

Suppose three kinematic GPS antennas are mounted on the aircraft at the front, the back and the right wing (denoted as f, b, w), so that the y components of the coordinates of front and back antennas in the body frame are zero, i.e., $y_f^b = y_b^b = 0$, and x, z components of the coordinates of the wing antenna in the body frame are zero, i.e., $x_w^b = z_w^b = 0$. Then the coordinates of three antennas in body fixed frame are $P_f(x_f^b, 0, z_f^b)$, $P_b(x_b^b, 0, z_b^b)$, and $P_w(0, y_w^b, 0)$. Because the antennas are mounted as above supposed and because the flight-state is computed by the positions of three antennas, there are pitch and roll correction angles that can be computed from the three coordinates by

$$\tan(\theta_0) = \frac{z_f^b - z_b^b}{x_f^b - x_b^b} \quad \text{and} \tag{10.10}$$

$$\tan(\phi_0) = -\frac{z_0}{y_w^b}, \tag{10.11}$$

where

$$z_0 = z_f^b - x_f^b \tan(\theta_0). \tag{10.12}$$

Through kinematic positioning and coordinate transformation, one has the coordinates of the three points in the local horizontal frame $P_f(x_f, y_f, z_f)$, $P_b(x_b, y_b, z_b)$, and $P_w(x_w, y_w, z_w)$. Then the three flight-state monitoring angles can be computed by

$$\tan(\psi) = \frac{y_f - y_b}{x_f - x_b}, \tag{10.13}$$

$$\tan(\theta - \theta_0) = \frac{z_f - z_b}{S}, \tag{10.14}$$

$$S = \sqrt{(x_f - x_b)^2 + (y_f - y_b)^2}, \tag{10.15}$$

$$\tan(\phi - \phi_0) = \frac{z_w - z_0}{s} \quad \text{and} \tag{10.16}$$

$$s = \sqrt{(x_w - x_0)^2 + (y_w - y_0)^2}, \tag{10.17}$$

where $\sqrt{\quad}$ is the squares root operator and

$$x_0 = x_f - (x_f - x_b)K, \quad (10.18)$$

$$y_0 = y_f - (y_f - y_b)K, \quad (10.19)$$

$$z_0 = z_f - (z_f - z_b)K \quad \text{and} \quad (10.20)$$

$$K = \frac{x_f^b}{x_f^b - x_b^b}. \quad (10.21)$$

Comparisons of numerical GPS flight-state monitoring results are made with the results of INS. It is possible to use GPS to determine the heading with an accuracy up to 0.1 degree, and pitch and roll up to 0.2 degree. In this case, the distances between the three antennas were 5.224 m, 5.510 m and 4.798 m.

10.2.4 Results, Precision Estimation and Comparisons

Examples demonstrating the above-mentioned methods are given through kinematic/static processing a set of kinematic/static GPS data collected on the 3 October 1997 at the islands of Portugal in the Atlantic Ocean within the Azores campaign. Two reference stations (Faim and Flor) served as static references and have a distance of about 239.4 km. Three antennas are fixed at the front, the back and the wing of the aircraft for determining the flight-state. The distances between the baselines of front-back, front-wing, and back-wing are 5.224, 5.510, and 4.798 meters, respectively. The flight time is about 4 hours. The length of the area is about 400 km (Fig. 10.11). The height of the flight is about 400 meters (Fig. 10.12).

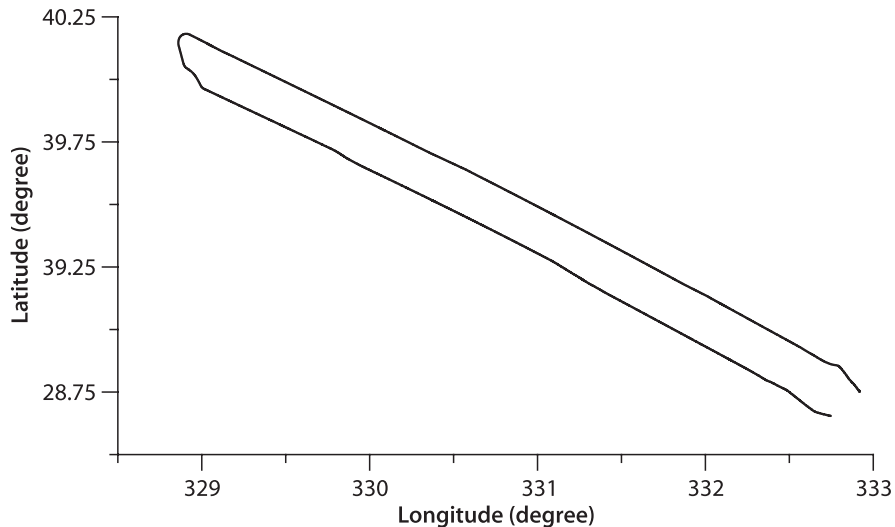


Fig. 10.11. One flight trace determined by kinematic GPS

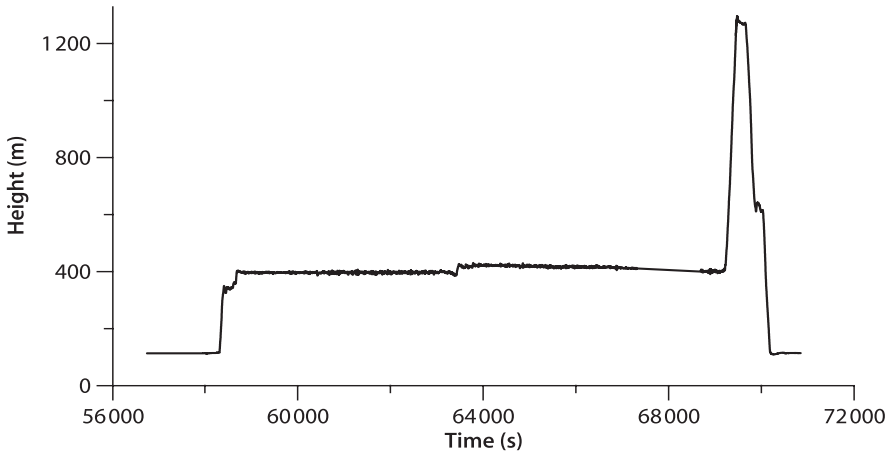


Fig. 10.12. Height profile of one flight determined by kinematic GPS

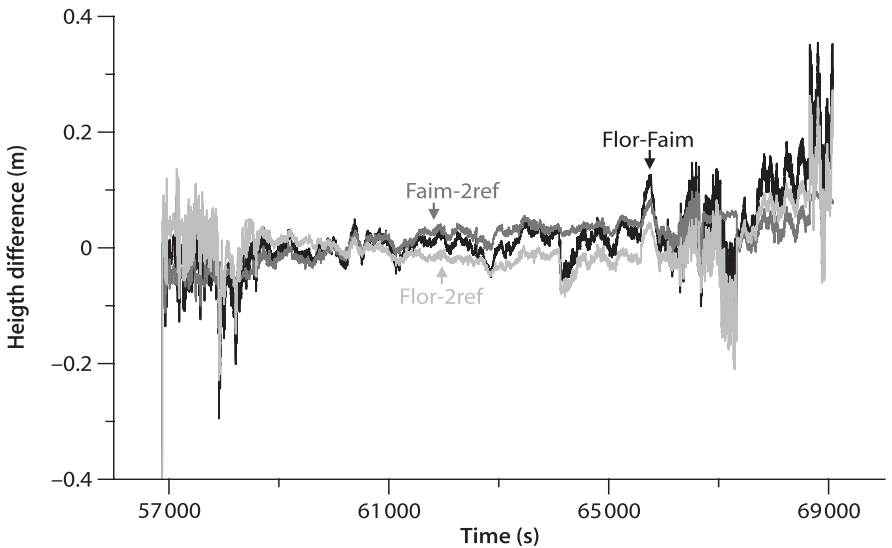


Fig. 10.13. Height differences caused by static references

10.2.4.1
Multiple Static References for Kinematic Positioning

The flight trajectory determined by using multiple references is a kind of weighted average path of the trajectories determined by using a single reference separately. The heights of the front antenna are determined by using a single reference and multiple references, respectively. The height differences of Flor-Faim, Flor-2ref, and Faim-2ref are given in Fig. 10.13 with dark, light, and medium grey lines. Where Flor-Faim means the height differences between the results obtained by using Flor and Faim as a static reference sepa-

rately, 2ref means two references are used. The statistics of the differences are given in Table 10.1 (units: cm). It shows that the multiple references helped to stabilise the results.

10.2.4.2

Ambiguity of Multiple Static References as a Condition for Kinematic Positioning

In the case of multiple static references, a static solution between the static references can be made for obtaining the static ambiguity vector. Such a vector usually can be obtained with excellent quality. By introducing such results as conditions for kinematic positioning, the accuracy of the position solution can be modified. The differences of the heights of the front antenna determined by using multiple references with and without using static ambiguities as conditions are given in Fig. 10.14. The average and standard deviation of the differences are 27.07 and 4.34 cm, respectively. These have shown that the multiple static conditions have helped to modify the results. A change of ambiguity not only caused a bias, but also a variation in the results.

Using multiple static references and introducing the static ambiguities as conditions, accuracy of the kinematic positioning can rise significantly. However, the airborne altimetry results have shown that the GPS height solution still has a bias. Therefore, airport height information is introduced as a condition for modifying ambiguity resolution and eliminating the height bias of the GPS solution. To introduce tropospheric parameters for the aircraft, statically determined parameters and the vertical temperature gradient have been used.

Table 10.1.
Statistics of the differences of
the heights determined

Height differences	Average	Deviation
Flor-2ref	1.62	3.52
Faim-2ref	-0.27	4.76
Flor-Faim	1.89	6.27

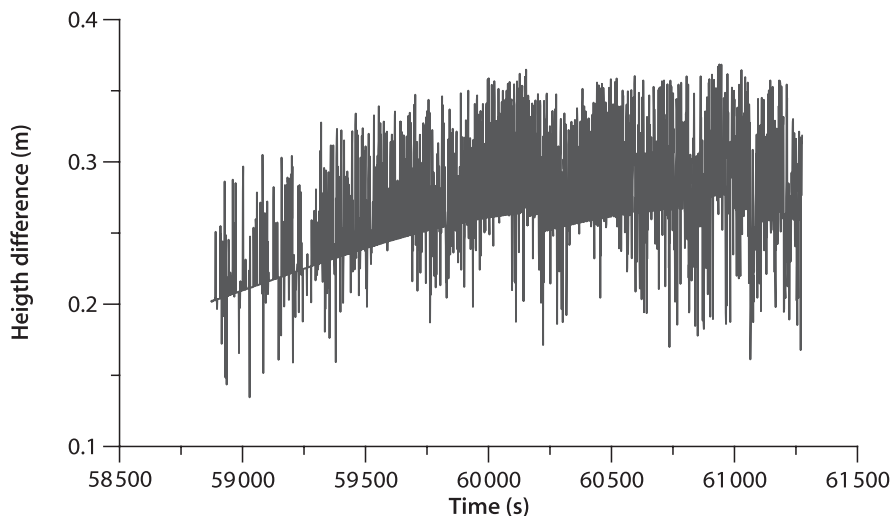


Fig. 10.14. Height differences caused by static references

10.2.4.3

Multiple Kinematic GPS for Flight-State Monitoring and its Comparison with INS

GPS determined heading, pitch and roll are given in Fig. 10.15 and 10.16 (with dark and light lines), respectively. Comparisons are made with the results of INS. The differences of the flight-state angles determined by GPS and INS are given in Fig. 10.17. The differences of the heading, pitch and roll are represented with dark, medium and light lines, respectively.

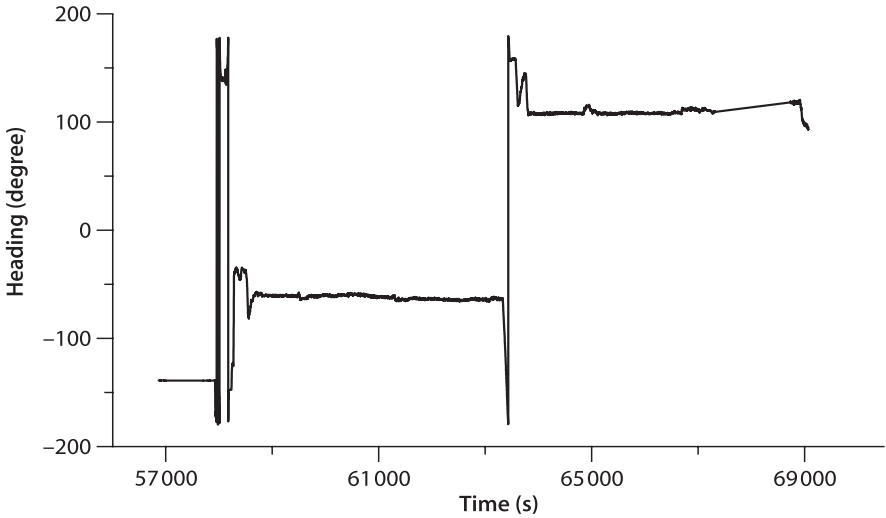


Fig. 10.15. Heading determined by GPS

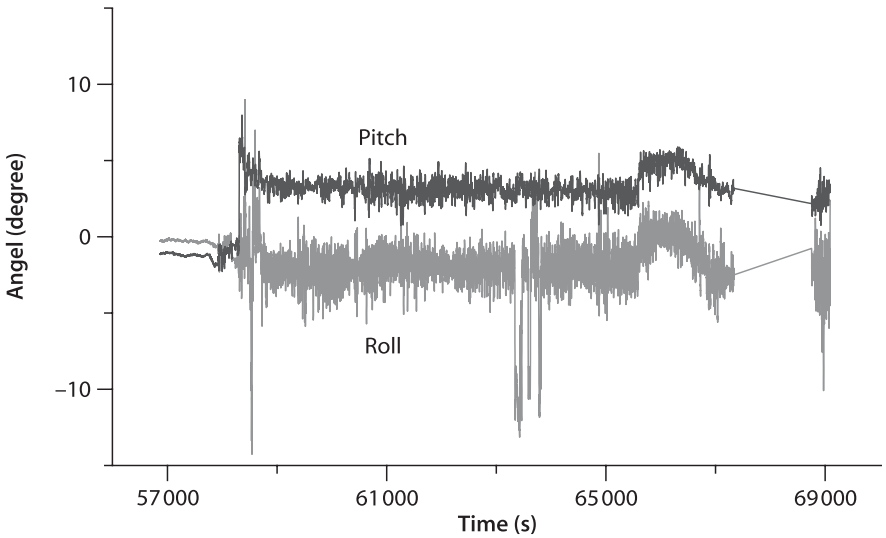


Fig. 10.16. Pitch and roll determined by GPS

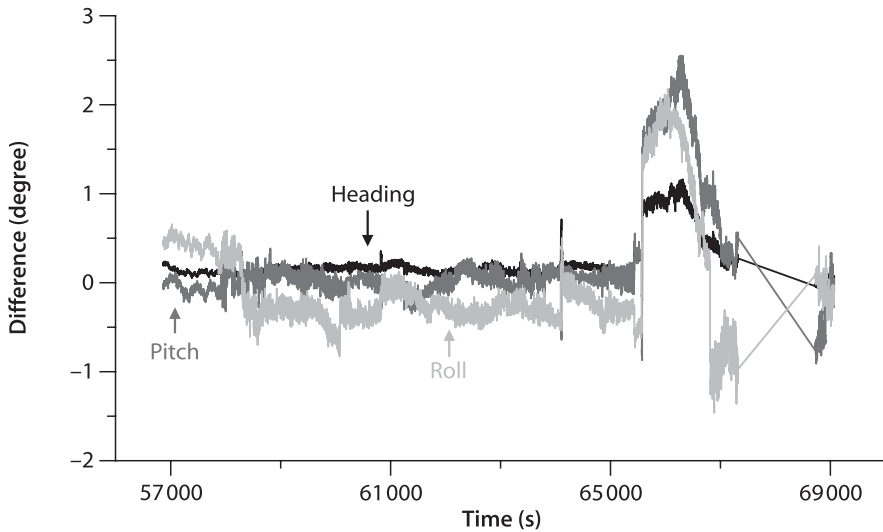


Fig. 10.17. Differences of flight state determined by GPS and INS

Table 10.2.

Statistics of the differences of the flight-state angles determined by GPS and INS

Differences of	Average	Deviation
Heading	0.230	0.238
Pitch	0.233	0.596
Roll	-0.249	0.612

light grey lines, respectively. The statistics of differences of the heading, pitch and roll are given in Table 10.2 (units: degrees). The larger deviations of the pitch and roll are due to larger uncertainties of the height components determined by GPS. Considering the large deviation around epoch 66 000 and the data gap in INS around epoch 68 000, it is possible to use GPS to determine the heading with accuracy up to 0.1 degree and pitch and roll up to 0.2 degree.

10.2.4.4

Static GPS Data Kinematic Processing

Static GPS data kinematic processing is one of the methods used to check the reliability of the GPS software working in a kinematic module. Such static data kinematic processing has been used for studying Earth tide effects (Xu and Knudsen 2000) and ocean loading tide effects. Faim has been used as a reference, and the position of Flor has been solved with static and kinematic modules. The static height of Flor is 98.257 m. The kinematic height average is 98.272 m, and its standard deviation is 3.8 cm. This indicates that kinematic data processing can reach an accuracy of about 4 cm with a baseline length of about 240 km. It seems that the results are very good; however, the kinematic height graphic (see Fig. 10.18) shows a clear ambiguity problem in kinematic data processing. As soon as a satellite goes up or down, a jump will occur in the solution trajectory.

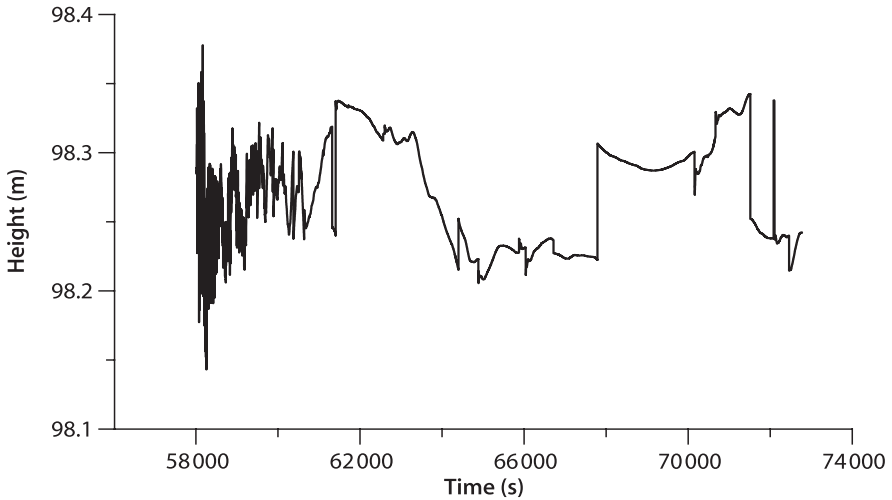


Fig. 10.18. Height changes by static data kinematic processing

Table 10.3. Statistics of the differences of the velocity

Velocity difference	dVs	dVe	dVh
Average	0.03	-0.01	-0.06
Deviation	0.27	0.17	0.53

10.2.4.5 Doppler Velocity Comparisons

Previous study (Xu et al. 1997) has shown that the velocity solution derived from Doppler measurements has a very high accuracy. It seems that the velocity solutions are independent from the static references. A statistic analysis of the differences of the velocity solved by using a different static reference (Flor or Faim) is given in Table 10.3 (units: cm s^{-1}), which confirms again the previous conclusion. The nominal flight velocity is about 80 m s^{-1} in horizontal. In the vertical component, the maximum velocity is about 5 m s^{-1} .

10.2.5 Conclusions

GPS research during the AGMASCO project has concluded that GPS is able to be used for airborne kinematic positioning and flight-state monitoring to fulfil the needs of navigating a remote sensing system for applications in aerogravimetry and oceanography.

A methodology has been proposed for precise kinematic GPS positioning that addresses the following issues:

- Using IGS stations to obtain precise reference coordinates, and introducing Earth tide and ocean loading tide corrections;

- Introducing multiple static reference receivers, and using static ambiguity solution as conditions;
- Introducing the initial height information as a condition, and introducing the tropospheric model to the aircraft kinematic GPS receivers; and
- Modelling the higher order ionospheric effects, and using the general method of ambiguity searching in coordinate and ambiguity domains.

For flight-state monitoring, the kinematic reference and data of the single frequency L1 are used. Known distances between the multiple kinematic antennas are used as additional constraints.

Results have shown adequate performance of this methodology.